

Strong-field ionization of linear molecules by a bicircular laser field: Symmetry considerationsA. Gazibegović-Busuladžić,¹ M. Busuladžić,^{1,2} E. Hasović,¹ W. Becker,^{3,4} and D. B. Milošević^{1,3,5,*}¹*Faculty of Science, University of Sarajevo, Zmaja od Bosne 35, 71000 Sarajevo, Bosnia and Herzegovina*²*Faculty of Medicine, University of Sarajevo, Čekaluša 90, 71000 Sarajevo, Bosnia and Herzegovina*³*Max-Born-Institut, Max-Born-Strasse 2a, 12489 Berlin, Germany*⁴*National Research Nuclear University MEPhI, Kashirskoe Shosse 31, 115409 Moscow, Russia*⁵*Academy of Sciences and Arts of Bosnia and Herzegovina, Bistrik 7, 71000 Sarajevo, Bosnia and Herzegovina*

(Received 3 February 2018; revised manuscript received 11 April 2018; published 30 April 2018)

Using the improved molecular strong-field approximation, we investigate (high-order) above-threshold ionization [(H)ATI] of various linear polyatomic molecules by a two-color laser field of frequencies $r\omega$ and $s\omega$ (with integer numbers r and s) having coplanar counter-rotating circularly polarized components (a so-called bicircular field). Reflection and rotational symmetries for molecules aligned in the laser-field polarization plane, analyzed for diatomic homonuclear molecules in *Phys. Rev. A* **95**, 033411 (2017), are now considered for diatomic heteronuclear molecules and symmetric and asymmetric linear triatomic molecules. There are additional rotational symmetries for (H)ATI spectra of symmetric linear molecules compared to (H)ATI spectra of the asymmetric ones. It is shown that these symmetries manifest themselves differently for $r + s$ odd and $r + s$ even. For example, HATI spectra for symmetric molecules with $r + s$ even obey inversion symmetry. For ATI spectra of linear molecules, reflection symmetry appears only for certain molecular orientation angles $\pm 90^\circ - jr180^\circ/(r + s)$ (j integer). For symmetric linear molecules, reflection symmetry appears also for the angles $-jr180^\circ/(r + s)$. For perpendicular orientation of molecules with respect to the laser-field polarization plane, the HATI spectra are very similar to those of the atomic targets, i.e., both spectra are characterized by the same type of the $(r + s)$ -fold symmetry.

DOI: [10.1103/PhysRevA.97.043432](https://doi.org/10.1103/PhysRevA.97.043432)**I. INTRODUCTION**

Nonlinear laser-induced processes such as high-order harmonic generation and high-order above-threshold ionization, generated by a so-called bicircular laser field, have been among the most popular and most investigated phenomena in laser science and strong-field physics for the past few years. A bicircular laser field consists of two coplanar counter-rotating circularly polarized fields having different angular frequencies. Such fields were already considered more than 20 years ago [1–3]: High-order harmonic generation from atomic targets induced by such a field was investigated using S -matrix theory and the strong-field approximation in Refs. [4–8]. This process has again attracted attention after the experimental confirmation [9] that the generated high harmonics are circularly polarized. Such harmonics will have many applications, which triggered a series of papers devoted to processes in bicircular fields [10–28].

In this paper, we are interested in molecular strong-field ionization induced by a bicircular laser field. This process is called above-threshold ionization (ATI) since more photons are absorbed from the laser field than is necessary for ionization. If the laser field and the molecular parameters are such that the Keldysh parameter $\gamma = \sqrt{I_p/(2U_p)}$ [29] (with I_p the ionization potential and U_p the ponderomotive energy of the free electron in the laser field) is small, then the dominant mechanism is tunneling ionization. The theory that we will use in the

present paper is applicable also in the regime where $\gamma \approx 1$ and multiphoton ionization appears. If the liberated electron returns to the parent molecular ion and elastically scatters off it, reaching the detector with a much higher energy than otherwise, then this process is called high-order ATI or HATI. Generally, the rescattered electrons contribute to the high-energy part of the electron spectrum, which forms a plateau region wherein the photoelectron (HATI) yield is practically constant but much lower than that of the ATI process. This plateau is terminated by an abrupt cutoff (for more details, see, for example, the review article [34] and references therein). Having in mind that the rescattered electron is described by a wave packet and that the rescattering can be in any direction, i.e., that one should consider the angular dependence of the electron energy spectra, the HATI process is sometimes called laser-induced electron diffraction [30–33].

Bicircular (H)ATI from atomic targets and a very similar process—above-threshold detachment (ATD) from negative ions—were analyzed in Refs. [35–37]. More recently, bicircular (H)ATI from inert gases was investigated in Refs. [38–41], while the corresponding (H)ATD process was analyzed in Ref. [42]. By analyzing results from a numerical solution of the time-dependent Schrödinger equation for atoms in few-cycle bicircular laser pulses, it was shown that HATI momentum spectra can be used to extract accurate elastic-scattering differential cross sections of the target ion [43]. Channel-closing effects in strong-field ionization by a bicircular field were recently considered in [44].

Let us now briefly comment on our theory of molecular strong-field ionization, which will be used in this paper. To

*Corresponding author: milo@bih.net.ba

describe direct ionization of diatomic molecules, we have developed a theory that we call the modified molecular strong-field approximation, or MSFA [45,46]. Using this theoretical approach, experimental data for the low-energy part of the electron spectrum were simulated, and we confirmed key features of the direct ATI molecular spectra [47]. Moreover, suppression in the ATI spectra of the O_2 molecule was found [46]. This confirms that our theory is able to reproduce available experimental data for ATI of diatomic molecules. Our next step in the development of the MSFA theory was to include an additional interaction of the ionized electron with the molecular centers [48–51]. We named this theory the improved MSFA (IMSFA). The theory was formulated for a general electric-field vector $\mathbf{E}(t)$ and applied to the case of a linearly polarized field [48,49] and to the more general cases of an elliptically [50] and a circularly polarized field [51]. Similar considerations that take into account the rescattering process on heteronuclear diatomic molecules as well as polyatomic molecules were presented in Refs. [52–54]. We were again able to reproduce the key features observed in experimental data for molecular HATI [55–59] for both long and few-cycle laser pulses.

There are a few papers devoted to molecular HATI generated by a bicircular laser field. In our previously published paper, we extended our theoretical approach from atomic HATI [40] to molecules [60]. For this purpose, we have also used the IMSFA theory mentioned in the previous paragraph. We considered the general symmetries of homonuclear molecules and of the applied bicircular laser field. In the mentioned paper, we were able to identify four symmetries (two rotational and two reflection symmetries), which are satisfied by the ATI spectra of homonuclear diatomic molecules. It is important to stress that the rotational symmetries, in contrast to the reflection symmetries, are valid both for the direct ATI electrons and for the rescattered HATI electrons. All symmetries mentioned were illustrated using the N_2 molecule as the target and an ω - 2ω bicircular laser field.

Now, our aim is to analyze the behavior of more complex molecules in a bicircular laser field and to compare their HATI spectra and the corresponding symmetries with those obtained for homonuclear molecules. More precisely, we consider the HATI process for different diatomic molecular species (O_2 , N_2 , and CO) and the polyatomic linear molecules CO_2 and OCS. We also present more results for homonuclear diatomic molecules characterized by different symmetries of their highest occupied molecular orbital and for various combinations of angular frequencies of the bicircular $r\omega$ - $s\omega$ field, with the integer numbers r and s and the fundamental frequency ω . We will also consider the influence of molecular alignment on bicircular HATI spectra.

This paper is organized as follows. In Sec. II, we define our counter-rotating bicircular field and the geometry of the molecular HATI process, and we present our IMSFA theory for heteronuclear and polyatomic molecules and a bicircular field. In Sec. IV, we consider the general rotational symmetries of the molecules and the applied bicircular laser field and the corresponding HATI spectra. Numerical results, which confirm the presented considerations, are also given. In Sec. V, the reflection symmetries of the ATI spectra for the considered molecules are analyzed and the corresponding numerical

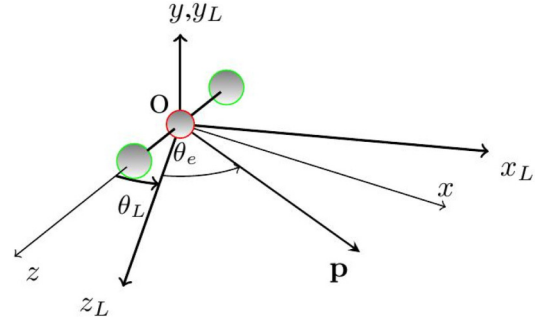


FIG. 1. Schematic presentation of the coordinate systems used in the paper. The linear molecule is along the z axis in the $Ozxy$ coordinate system. The laser field lies in the Oz_Lx_L plane of the $Oz_Lx_Ly_L$ coordinate system, which is rotated around the $y = y_L$ axis by the angle θ_L with respect to the $Ozxy$ coordinate system. The direction of the emitted-electron momentum \mathbf{p} is determined by the angle θ_e with respect to the z_L axis.

results are presented. Finally, our conclusions are given in Sec. VI. We use the atomic system of units.

II. NOTATIONS AND THEORY

For most calculations, we suppose that the laser field, the molecule, and the emitted electron all lie in the same plane (see Fig. 1). In the present paper, we consider only examples of diatomic and triatomic linear molecules. In our theoretical approach, a linear polyatomic molecule is modeled by an $(N + 1)$ -particle system, which consists of N heavy atomic (ionic) centers and one valence electron. We denote by $\mathbf{R} \equiv \{\mathbf{R}\} = (\mathbf{R}_1, \mathbf{R}_2, \dots, \mathbf{R}_{N-1})$ the set of relative coordinates of all atomic centers with respect to the center of mass. The vector $\mathbf{R}_N \equiv \mathbf{r}$ describes the relative motion of the electron (the notation of Refs. [54,61] is used). For linear molecules, all vectors from the set $\{\mathbf{R}\}$ are along the z axis. The laser field is defined in the coordinate system Oz_Lx_L , which is rotated with respect to the Ozx system by the angle θ_L around the $y = y_L$ axis, which is perpendicular to the polarization plane. The momentum \mathbf{p} of the emitted electron is in the direction determined by the angles θ_e in the Oz_Lx_L system and $\theta = \theta_L + \theta_e$ in the Ozx system (for a molecule aligned in the laser-field polarization plane). The unit vectors of the corresponding coordinate systems are related by

$$\hat{\mathbf{e}}_{Lz} = \hat{\mathbf{z}} \cos \theta_L + \hat{\mathbf{x}} \sin \theta_L, \quad \hat{\mathbf{e}}_{Lx} = -\hat{\mathbf{z}} \sin \theta_L + \hat{\mathbf{x}} \cos \theta_L. \quad (1)$$

We consider a bicircular field having the period T and the fundamental frequency $\omega = 2\pi/T$, with the electric-field vector [60]

$$\mathbf{E}(t) = \frac{E_L}{\sqrt{2}} \{ [\sin(r\omega t) + \sin(s\omega t)] \hat{\mathbf{e}}_{Lz} - [\cos(r\omega t) - \cos(s\omega t)] \hat{\mathbf{e}}_{Lx} \}. \quad (2)$$

We assume equal component strengths and fix the relative phases to zero ($E_1 = E_2 = E_L$, $\phi_1 = \phi_2 = 0$ compared with the notation of Ref. [40]). In Fig. 2, we present parametric plots of the ω - 2ω and ω - 3ω bicircular fields.

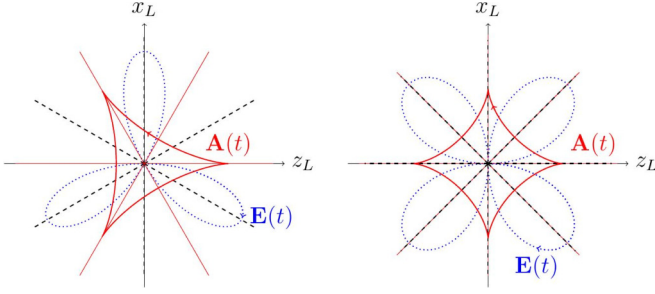


FIG. 2. Electric-field vector $\mathbf{E}(t)$ (blue dotted curves) and vector potential $\mathbf{A}(t)$ (red solid curves) of the bicircular field (2) for $r = 1$ and $s = 2$ (left panel) and for $r = 1$ and $s = 3$ (right panel). Each reflection axis of the electric field (dashed lines) is perpendicular to the corresponding reflection axis of the vector potential (red solid lines). For $r + s$ even, the reflection axes of the vector potential and the electric field coincide.

We use the improved molecular strong-field approximation to calculate the differential ionization rate for emission of an electron with final momentum \mathbf{p} :

$$w_{\mathbf{R}\mathbf{p}i}(n) = 2\pi p |T_{\mathbf{R}\mathbf{p}i}(n)|^2. \quad (3)$$

Here $n = n_1 r + n_2 s$, and n_1 photons of frequency $r\omega$ and n_2 photons of frequency $s\omega$ are absorbed from the bicircular field (2). In the IMSFA, the T -matrix element of the (H)ATI process can be written as

$$T_{\mathbf{R}\mathbf{p}i}(n) = \int_0^T \frac{dt}{T} [\mathcal{F}_{\mathbf{R}\mathbf{p}i}^{(0)}(t) + \mathcal{F}_{\mathbf{R}\mathbf{p}i}^{(1)}(t)] e^{i n \omega t + i \mathcal{U}(t)}, \quad (4)$$

with the time-periodic functions $\mathcal{F}_{\mathbf{R}\mathbf{p}i}^{(j)}(t)$, $j = 0, 1$, and $\mathcal{U}(t) = \mathbf{p} \cdot \boldsymbol{\alpha}(t) + \int^t d\tau \mathbf{A}^2(\tau)/2 - U_p t$, where $\boldsymbol{\alpha}(t) = \int^t d\tau \mathbf{A}(\tau)$, U_p is the ponderomotive energy, and $\mathbf{A}(t) = -\int^t d\tau \mathbf{E}(\tau)$. The energy-conservation condition has the form $E_{\mathbf{p}} = \mathbf{p}^2/2 = n\omega - I_p - U_p$. For asymmetric molecules, the unperturbed ionization potential I_p should be replaced by $I_p - \Delta_S$, where Δ_S is the polarizability-induced Stark shift [52]. For our bicircular field, we have $\Delta_S = -E_L^2(\alpha_{\parallel} + \alpha_{\perp})/4$, where α_{\parallel} and α_{\perp} , respectively, are the polarizability parallel and perpendicular to the molecular axis.

The zeroth-order term, which corresponds to the direct ATI electrons, for neutral polyatomic molecules is described by the matrix element [61]

$$\mathcal{F}_{\mathbf{R}\mathbf{p}i}^{(0)}(t) = \sum_{j=1}^N f(\boldsymbol{\rho}_j, t) e^{-i\mathbf{p} \cdot \boldsymbol{\rho}_j} \sum_a c_{ja} (\mathbf{p} + \mathbf{A}(t) | \mathbf{E}(t) \cdot \mathbf{r} | \psi_a), \quad (5)$$

where the c_{ja} are the coefficients of an expansion of the molecular electronic ground-state wave function in a linear combination of the atomic orbitals ψ_a . For symmetric linear molecules and dressed atomic orbitals, we have $f(\boldsymbol{\rho}_j, t) = 1$, while for asymmetric linear molecules and dressing of the whole molecular orbital we have $f(\boldsymbol{\rho}_j, t) = \exp\{i[\mu_S(t) + \alpha_S(t) - \mathbf{A}(t) \cdot \boldsymbol{\rho}_j]\}$. The two time-dependent terms, $\mu_S(t) = \int^t \boldsymbol{\mu} \cdot \mathbf{E}(t') dt'$ and $\alpha_S(t) = \int^t [\alpha_{\parallel} E_{\parallel}^2(t') + \alpha_{\perp} E_{\perp}^2(t')] dt'/2 + \Delta_S t$, enrich the oscillatory structure of the spectra [52,53]. Here $\boldsymbol{\mu} = -\mu \hat{\mathbf{z}}$ is the molecular dipole and $E_{\parallel}(t)$ [$E_{\perp}(t)$] is the electric-field

TABLE I. Ionization potential I_p and the Keldysh parameter γ for the molecules considered in the paper. The Keldysh parameter is calculated for a bicircular field with $r = 1$ and $s = 2$, equal component intensities $E_1^2 = E_2^2 = 1 \times 10^{14}$ W/cm², and the fundamental wavelength of 800 nm.

Molecule	N ₂	O ₂	CO	CO ₂	OCS
I_p (eV)	15.58	12.03	14.014	13.777	11.19
γ	1.0212	0.8974	0.9685	0.9603	0.8655

vector parallel (perpendicular) to the molecular axis. The coordinates $\boldsymbol{\rho}_j$ are defined in Refs. [54,61] as linear combinations of the relative coordinates $\{\mathbf{R}\}$. For $N = 2$, we have $\boldsymbol{\rho}_j = -(q - \lambda)\mathbf{R}_1/2$, where $\lambda = (m_1 - m_2)/(m_1 + m_2)$ is the mass asymmetry parameter and $q = +1$ for $j = 1$ and $q = -1$ for $j = 2$. In this case, the sum over j in Eq. (5) is replaced by the sum over $q = \pm 1$. For $\lambda = 0$, this reduces to the result known for homonuclear diatomic molecules from Ref. [45].

The first-order term, which corresponds to the rescattered electrons, for neutral polyatomic molecules has the form

$$\begin{aligned} \mathcal{F}_{\mathbf{R}\mathbf{p}i}^{(1)}(t) = & -i e^{-i S_{\mathbf{k}_{\text{st}}}(t)} \int_0^{\infty} d\tau \left(\frac{2\pi}{i\tau}\right)^{3/2} e^{i[S_{\mathbf{k}_{\text{st}}}(t') - (I_p - \Delta_S)\tau]} \\ & \times \sum_{j=1}^N e^{i\mathbf{K} \cdot \boldsymbol{\rho}_j} V_{\mathbf{e}\mathbf{K}}^j \sum_{l=1}^N f(\boldsymbol{\rho}_l, t') e^{-i\mathbf{k}_{\text{st}} \cdot \boldsymbol{\rho}_l} \\ & \times \sum_a c_{la} (\mathbf{k}_{\text{st}} + \mathbf{A}(t') | \mathbf{E}(t') \cdot \mathbf{r} | \psi_a), \end{aligned} \quad (6)$$

with $t' = t - \tau$, $\mathbf{K} = \mathbf{k}_{\text{st}} - \mathbf{p}$, $\mathbf{k}_{\text{st}} = \int_t^{t'} dt'' \mathbf{A}(t'')/\tau$ the stationary electron momentum, and $S_{\mathbf{k}}(t) = \int^t dt' [\mathbf{k} + \mathbf{A}(t')]^2/2$. In the above equation, $V_{\mathbf{e}\mathbf{K}}^j$ is the Fourier transform of the rescattering potential at the atomic (ionic) j th center.

III. EXAMPLES OF ATI AND HATI SPECTRA FOR LINEAR MOLECULES

Before analyzing rotational and reflection symmetries of the photoelectron spectra, we fix the molecular and laser-field parameters, which we use in the paper, and present examples of the ATI and HATI spectra for various linear molecules. Spectra calculated using Eqs. (3) and (4) will be referred to as HATI spectra. If we neglect $\mathcal{F}_{\mathbf{R}\mathbf{p}i}^{(1)}(t)$ in Eq. (4), i.e., if we take into account only the direct electrons, the corresponding spectra will be called ATI spectra.

In all examples in the present paper, we fix the laser intensity to $E_L^2 = 1 \times 10^{14}$ W/cm². For this intensity, the rescattering effects are clearly visible and the saturation of ionization is not too high (for the Ar atom, which is the companion of the N₂ molecule, the saturation intensity is 2×10^{14} W/cm², while for the Xe atom, which is the companion of the O₂ molecule, it is 7×10^{13} W/cm² [62]). The fundamental laser wavelength is 800 nm, except in Figs. 7 and 14. The values of the ionization potential and the Keldysh parameter for this intensity and wavelength are presented in Table I for the case in which $r = 1$ and $s = 2$. The corresponding ponderomotive energy is $U_p = 7.47$ eV, while for $r = 1$ and $s = 3$ it is $U_p = 6.64$ eV. These parameters are chosen for simplicity, but it should be

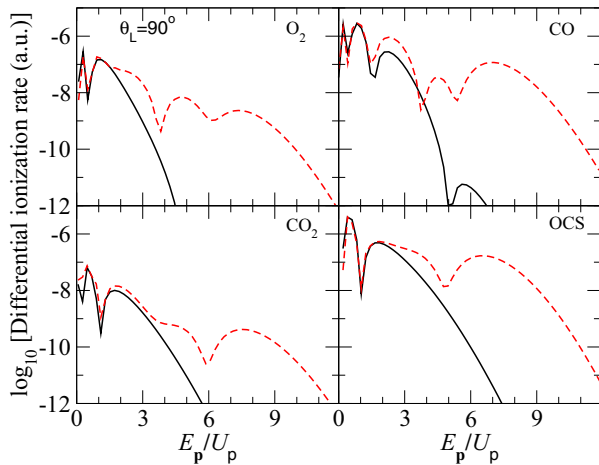


FIG. 3. Electron ATI (black solid line) and HATI spectra (red dashed line), obtained using the IMSFA, for the O_2 , CO , CO_2 , and OCS molecules, laser intensity $E_L^2 = 1 \times 10^{14}$ W/cm^2 , $r = 1$, $s = 2$, and the fundamental wavelength of 800 nm. The electron emission angle is $\theta_e = 180^\circ$ and the molecular orientation angle is $\theta_L = 90^\circ$.

mentioned that the symmetries considered in our paper do not depend on the chosen laser-field intensity.

In Fig. 3, we present electron ATI and HATI spectra for various molecules. The electron emission angle with respect to the laser-field coordinate system is chosen to be $\theta_e = 180^\circ$, which gives a maximal length of the rescattered-electron plateau length (such maximal length is also obtained for $\theta_e = \pm 60^\circ$). The molecular-orientation angle is $\theta_L = 90^\circ$. From Fig. 3, one can notice that the direct ATI electrons are dominant for $E_p < 2U_p$. The ATI differential ionization rate exponentially decreases for higher energies. The HATI spectra exhibit a plateau, which finishes with a cutoff near $E_p = 8U_p$. The presented photoelectron energy spectra for molecules are similar to those of atoms.

Differences between the atomic and molecular spectra appear in the angular distributions. It is known that the atomic photoelectron-momentum distribution for the $\omega-2\omega$ bicircular field exhibits threefold symmetry [40]. For molecules this symmetry is violated. The symmetry breaking is caused by the interference of contributions to ionization from the different atomic centers of the molecule. In Figs. 4 and 5, we present two examples that confirm this. Polar diagrams of the HATI photoelectron angular distributions are shown for four molecules (O_2 , CO , CO_2 , and OCS) and two molecular orientations: $\theta_L = 0^\circ$ (Fig. 4) and $\theta_L = 60^\circ$ (Fig. 5). The parameters of the bicircular field are the same as in Fig. 3 and the photoelectron energy is fixed to approximately $8U_p$ (59.75 eV). This energy is chosen as an energy near the high-energy cutoff, where only rescattered electrons contribute. The complete HATI electron-momentum distributions for these molecular orientations and for the CO_2 and CO molecules are presented in Figs. 6 and 9, respectively. The photoelectron energy of $8U_p$ corresponds to a momentum of approximately 2.12 a.u. Comparing the angular photoelectron distributions presented in Figs. 4 and 5, it is obvious that they are different for different molecular orientations. It is interesting to notice that the angular distributions for $\theta_L = 60^\circ$ for the O_2 and CO_2 molecules are the same as the corresponding angular

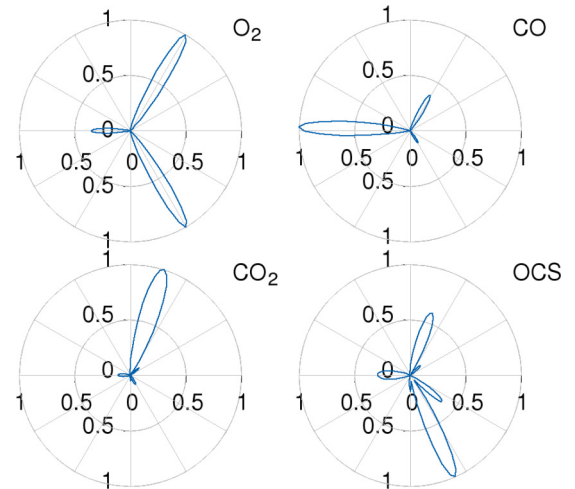


FIG. 4. Differential ionization rate for electrons with kinetic energy of (approximately) $8U_p$ for the molecular orientation $\theta_L = 0^\circ$ normalized to 1, which corresponds to the maximal values 3×10^{-7} a.u. for O_2 , 8.25×10^{-9} a.u. for CO , 1.39×10^{-9} a.u. for CO_2 , and 6.64×10^{-8} a.u. for the OCS molecule. The laser-field parameters are the same as in Fig. 3.

distributions for $\theta_L = 0^\circ$ if rotated by 120° . This is not the case for the CO and OCS molecules. We will explain this in Sec. IV.

IV. ROTATIONAL SYMMETRIES

The bicircular field (2) obeys the following dynamical symmetry [40]:

$$\mathbf{E}'(t) \equiv R_y(\alpha_{j_1})\mathbf{E}(t) = \mathbf{E}(t + \tau_{j_1}),$$

$$\tau_{j_1} = \frac{j_1 T}{r+s}, \quad \alpha_{j_1} = -\frac{r}{r+s} j_1 2\pi, \quad j_1 = \text{integer}. \quad (7)$$

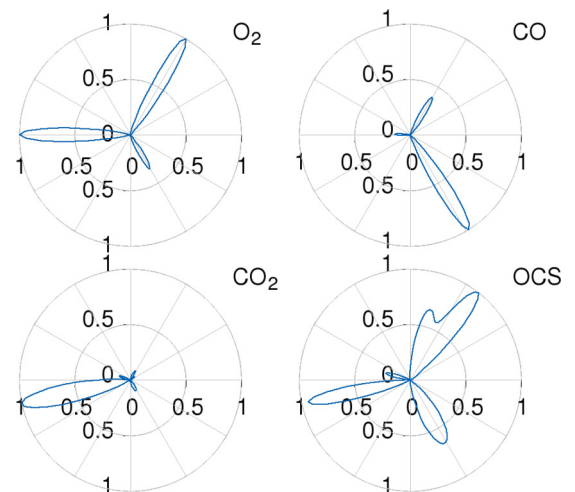


FIG. 5. Same as in Fig. 4, but for the molecular orientation $\theta_L = 60^\circ$ and the following maxima of the differential ionization rate: 3×10^{-7} , 8×10^{-9} , 1.39×10^{-9} , and 4.28×10^{-8} a.u. for O_2 , CO , CO_2 , and OCS molecules, respectively.

The prime denotes rotation of the respective vector by the angle α_{j_1} about the y axis, which is mediated by the 2×2 rotation matrix $R_y(\alpha_{j_1})$. A rotation by the angle $\alpha_{j_1} = -r\omega\tau_{j_1}$ about the y axis is equivalent to a translation in time by τ_{j_1} . We associate the index j_1 with the rotational symmetry (7). The index j_2 will be used for specific rotations (by the angles $j_2 180^\circ$) of symmetric linear molecules, while the index j_3 will be reserved to describe reflection symmetries in the next section.

We consider linear molecules that lie in the polarization plane of the laser field. We then have $y \parallel y_L$, i.e., the y axes of the two coordinate systems introduced above coincide; cf. Fig. 1. Due to Eq. (7), the HATI spectra for (different) molecular orientations θ_L and $\theta_L - \alpha_{j_1}$ transform into each other upon rotation by the angle α_{j_1} . It can be shown that the differential ionization rate is invariant with respect to a simultaneous rotation of the vector \mathbf{p} and all vectors from the set $\{\mathbf{R}\}$ about the y axis by the angle α_{j_1} , with the laser electric-field vector fixed, regardless of the symmetry of the linear molecule. Therefore, we have

$$w_{\mathbf{R}'\mathbf{p}'i}(n) = w_{\mathbf{R}\mathbf{p}i}(n), \quad (8)$$

where the prime on i means that the molecular ground-state wave function is also rotated. This relation was derived in Ref. [60] for homonuclear diatomic molecules, but it is valid for arbitrary linear polyatomic molecules.

In general, linear molecules whose position in the zx plane is determined by the vectors from the set $\{\mathbf{R}\}$ are not invariant with respect to rotation about the y axis. In particular, diatomic heteronuclear or other asymmetric linear molecules, aligned in the polarization plane of the laser field, do not exhibit rotational symmetry. However, symmetric linear molecules are invariant with respect to rotation about the y axis by the angle $j_2 180^\circ$, where j_2 is an integer.

The above-mentioned two rotational symmetries were explored in detail in Ref. [60] for the case of homonuclear diatomic molecules. They also hold for the HATI spectra of symmetric linear molecules. A combination of these symmetries leads to the conclusion that the corresponding differential ionization rate is invariant with respect to the transformation [in contrast to Eq. (7), we express angles in degrees]

$$\begin{aligned} \theta &\rightarrow \theta + j_2 180^\circ, & \theta_L &\rightarrow \theta_L + j_2 180^\circ - \alpha_{j_1}, \\ \theta_e &\rightarrow \theta_e + \alpha_{j_1}, & \alpha_{j_1} &= -j_1 \frac{r}{r+s} 360^\circ, \end{aligned} \quad (9)$$

where j_1 and j_2 are integers, which can take the values $0, \pm 1, \pm 2, \dots$. If we fix $j_2 = 0$, i.e., consider only rotation by the angle α_{j_1} , the relation (9) is valid also for asymmetric molecules.

Let us now illustrate the symmetry (9) with a few examples. In Fig. 6, we show results for the triatomic symmetric CO_2 for $r = 1$ and $s = 2$. The spectra shown in the upper panel ($\theta_L = 0^\circ$), if rotated by 120° [for $j_1 = -1$, relation (9) gives $\theta_e \rightarrow \theta_e + 120^\circ$], are the same as those in the lower panel (for $j_2 = 1$, we have $\theta_L \rightarrow \theta_L + 180^\circ - 120^\circ = 60^\circ$). As the second example, we consider the homonuclear diatomic molecule O_2 for $r = 1$ and $s = 4$. The corresponding spectra for the two orientations $\theta_L = 0^\circ$ and 36° are presented in Fig. 7. It can be noticed that these spectra are related by a rotation. Namely, combining the rotation by 180° ($j_2 = 1$,

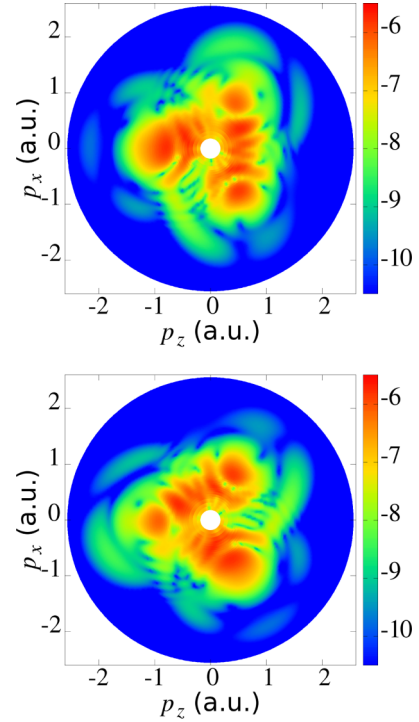


FIG. 6. Electron HATI spectra obtained using the IMSFA (both the direct and the rescattered electrons are included) for the CO_2 molecule, the laser intensity $E_L^2 = 1 \times 10^{14} \text{ W/cm}^2$, $r = 1$, $s = 2$, and the fundamental wavelength of 800 nm. The electron-momentum plane is defined with respect to the laser-field coordinate system: $p_z = p \cos \theta_e$, $p_x = p \sin \theta_e$. Upper panel: $\theta_L = 0^\circ$. Lower panel: $\theta_L = 60^\circ$. The logarithm of the differential ionization rate is presented using a false-color scale, which covers five orders of magnitude.

$\theta_L \rightarrow \theta_L + 180^\circ$) and the rotation of the bicircular field by $\alpha_{-2} = 2 \times 360^\circ / (1 + 4) = 144^\circ$ ($\theta_L \rightarrow \theta_L - 144^\circ$), the resulting combination leads to the transformation $\theta_L \rightarrow \theta_L + 180^\circ - 144^\circ = \theta_L + 36^\circ$, $\theta_e \rightarrow \theta_e + 144^\circ$.

The symmetry of HATI spectra for symmetric linear molecules can be further analyzed taking into account the parity of the number $r + s$. For symmetric molecules, the number j_2 from the transformation relation (9) is an arbitrary odd integer (for even j_2 nothing changes since the angles are defined modulo 2π) and we can write

$$\begin{aligned} j_2 180^\circ - \alpha_{j_1} &= -\alpha_{m'} + \frac{180^\circ}{r+s} \quad \text{for } r+s = 2k+1, \\ j_2 180^\circ - \alpha_{j_1} &= -\alpha_m \quad \text{for } r+s = 2k, \end{aligned} \quad (10)$$

where $m = j_1 + j_2 k / r$, $m' = j_1 + [j_2(2k+1) - 1] / (2r)$, and k are integers. If, for example, we choose $j_1 = -k$ and $j_2 = r$, we obtain $m = 0$, i.e., $\alpha_m = 0$. Therefore, for symmetric molecules, for $r + s$ even and for $m = 0$, the above transformation (9) takes the form

$$\begin{aligned} \theta &\rightarrow \theta + j_2 180^\circ, & \theta_L &\rightarrow \theta_L, \\ \theta_e &\rightarrow \theta_e + j_2 180^\circ \quad (r+s = \text{even}), \end{aligned} \quad (11)$$

which corresponds to the transformation $\mathbf{p} \rightarrow -\mathbf{p}$ with fixed positions of the molecule and the field. This *inversion symmetry* is clearly visible in both panels of Fig. 8. On the other hand,

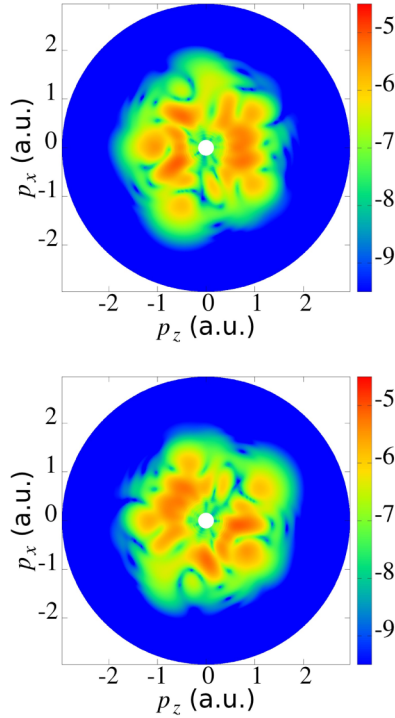


FIG. 7. Electron HATI spectra in the momentum plane obtained using the IMSFA for the O_2 molecule in the plane of the field, the laser intensity $E_L^2 = 1 \times 10^{14}$ W/cm 2 , $r = 1$, $s = 4$, and the fundamental wavelength of 1000 nm. Upper panel: alignment $\theta_L = 0^\circ$, lower panel: $\theta_L = 36^\circ$.

for $r + s$ odd, the smallest nontrivial (absolute) value of the angle $j_2 180^\circ - \alpha_{j_1}$ is $180^\circ/(r + s)$ [for $m' = 0$, i.e., for $j_1 = -[j_2(2k + 1) - 1]/(2r)$, in the first line of Eq. (10)]. Therefore, for symmetric molecules and $r + s = 2k + 1$ odd, there are suitable odd j_2 that yield the symmetry

$$\begin{aligned} \theta &\rightarrow \theta + j_2 180^\circ, & \theta_L &\rightarrow \theta_L + \frac{180^\circ}{r + s}, \\ \theta_e &\rightarrow \theta_e + \alpha_{-[j_2(r+s)-1]/(2r)} \quad (r + s = \text{odd}). \end{aligned} \quad (12)$$

This is illustrated in Fig. 6 for $\theta_L = 0^\circ \rightarrow \theta_L = 0^\circ + 60^\circ = 60^\circ$, $\theta_e \rightarrow \theta_e + \alpha_{-(3j_2-1)/2} = \theta_e + 120^\circ$ (for $j_2 = 1$). Analogously, for Fig. 7 we have $\theta_L = 0^\circ \rightarrow 36^\circ$ and $\theta_e \rightarrow \theta_e + \alpha_{-(5j_2-1)/2} = \theta_e + 144^\circ$ (for $j_2 = 1$). Generally, for symmetric molecules and $r + s$ odd, rotation of the molecule such that $\theta_L \rightarrow \theta_L - \alpha_{m'} + \frac{180^\circ}{r+s}$ leads to rotation of the HATI spectra in the momentum plane by the angle α_{j_1} so that $\theta_e \rightarrow \theta_e + \alpha_{j_1}$, where (with a suitable choice of odd j_2) $j_1 = m' - [j_2(r + s) - 1]/(2r)$ is an integer.

For asymmetric molecules such as, for example, heteronuclear diatomic molecules, we have only one rotational symmetry: the differential ionization rate is invariant with respect to the transformation (9) with $j_2 = 0$. This symmetry is illustrated in Fig. 9 for the CO molecule and a bicircular field with $r = 1$ and $s = 2$. For $\alpha_1 = -120^\circ$, one can see that the spectrum for $\theta_L = 120^\circ$ can be obtained from the spectrum for $\theta_L = 0^\circ$ by a rotation by the angle -120° , which corresponds to the transformation $\theta_e \rightarrow \theta_e - 120^\circ$ and is in accordance with the relation (9) for $j_2 = 0$. Unlike the case of the CO_2 molecule, presented in Fig. 6, for the CO

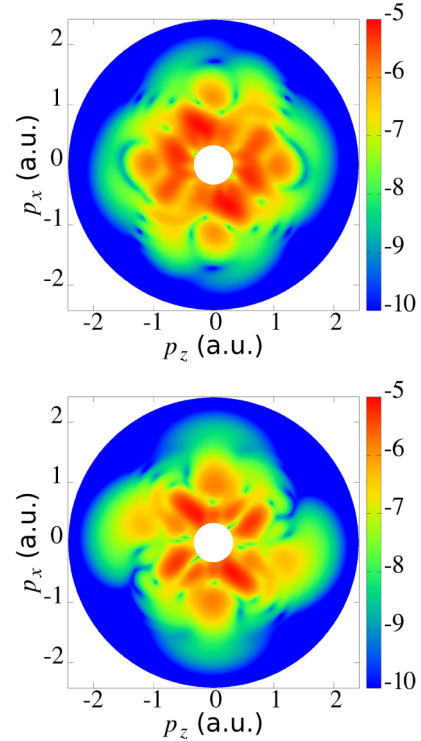


FIG. 8. Electron HATI spectra obtained using the IMSFA for the O_2 molecule, laser intensity given by $E_L^2 = 1 \times 10^{14}$ W/cm 2 , $r = 1$, $s = 3$, and the fundamental wavelength of 800 nm. Upper panel: $\theta_L = 45^\circ$. Lower panel: $\theta_L = 90^\circ$. The spectra satisfy inversion symmetry $\mathbf{p} \rightarrow -\mathbf{p}$ for $r + s$ even.

molecule in Fig. 9 there is no rotational symmetry between the spectra for $\theta_L = 0^\circ$ (top panel) and $\theta_L = 60^\circ$ (middle panel). In addition, due to the absence of the second rotational symmetry, for asymmetric linear molecules there is no different manifestation of the rotational symmetries for $r + s$ odd and $r + s$ even.

So far, we have considered rotational symmetry for molecules aligned in the polarization plane of the laser field. In general, relation (8) should hold for any molecular orientation provided that the rotation axis is perpendicular to the laser-field polarization plane. If the considered linear molecule is aligned perpendicular to this polarization plane, then the internuclear vectors \mathbf{R}_j , $j = 1, \dots, N - 1$, are invariant with respect to rotation about the axis perpendicular to the polarization plane of the field. In this case, the rotational symmetry of HATI spectra reduces to the atomic case [40], and molecular HATI spectra exhibit $(r + s)$ -fold rotational symmetry. This might be used as a tool to check the degree of linearity of certain molecules or to check the alignment for linear molecules. This is illustrated in Fig. 10 for the N_2 molecule. Though the spectrum exhibits $(r + s)$ -fold rotational symmetry just as in the atomic case, it also exhibits some features that are never present in the atomic case. For example, the origin of the spotlike minima that appear (in the upper panel in the area around $p_z = -0.5$ a.u., $p_x = 0$ a.u.; in the lower panel around $p_z = -0.75$ a.u., $p_x = 0.25$ a.u.) can be attributed to a destructive interference of the contributions of the two atoms to the direct ATI.

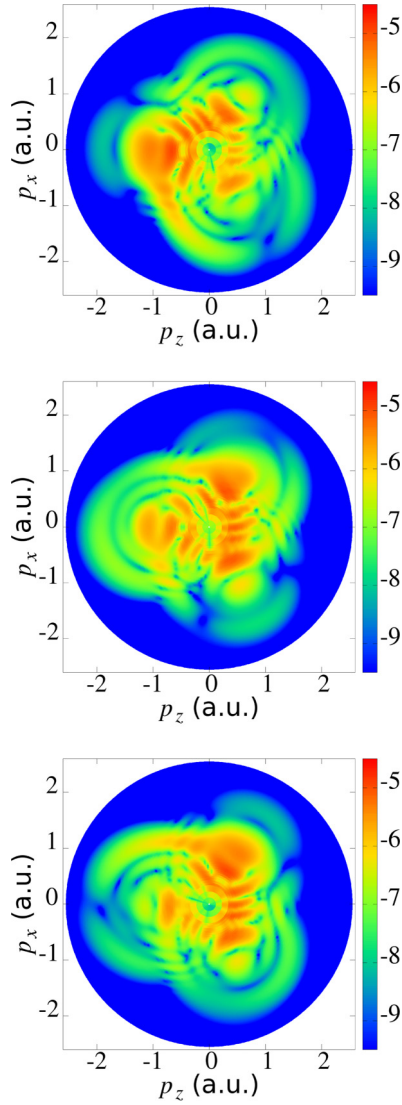


FIG. 9. Electron HATI spectra for the heteronuclear diatomic molecule CO and the same laser parameters as in Fig. 6. The orientation angles are $\theta_L = 0^\circ$ (top panel), $\theta_L = 60^\circ$ (middle panel), and $\theta_L = 120^\circ$ (bottom panel).

V. REFLECTION SYMMETRY

It was proven in Ref. [60] that the direct ATI spectra for homonuclear diatomic molecules obey reflection symmetries for two mutually perpendicular molecular orientations defined by the angles $\theta_L = 0^\circ$ and 90° . This is so for arbitrary symmetric linear molecules. An example is shown in the top and middle panels of Fig. 11 for the polyatomic symmetric molecule CO_2 . It is obvious that the presented spectra are invariant with respect to the transformation $\theta_e \rightarrow -\theta_e$. These reflection symmetries can be combined with the rotational symmetries described in the preceding section. For example, by rotating the spectrum shown in the bottom panel of Fig. 11 ($\theta_L = 30^\circ$) by the angle 120° , we obtain the spectrum presented in the middle panel ($\theta_L = 90^\circ$). This is in accordance with the relation (9) for $j_1 = -1$ and $j_2 = 1$.

It is also clear from the bottom panel of Fig. 11 that the direct ATI rate obeys reflection symmetry about the axis at

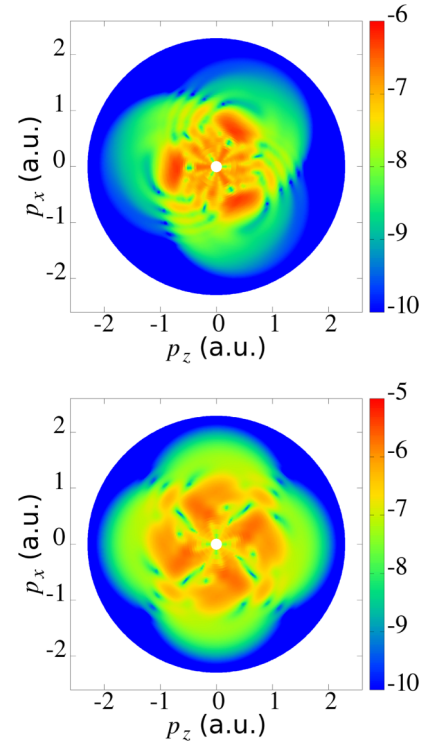


FIG. 10. Electron HATI spectra obtained using the IMSFA for the N_2 molecule oriented perpendicular to the polarization plane of the laser field, for laser-field intensity $E_L^2 = 1 \times 10^{14} \text{ W/cm}^2$, fundamental wavelength 800 nm, and for $r = 1, s = 2$ (upper panel), and $r = 1, s = 3$ (lower panel). The electron-momentum plane is defined with respect to the laser-field coordinate system: $p_z = p \cos \theta_e$, $p_x = p \sin \theta_e$.

the angle $\beta_1 = 60^\circ$ with respect to the positive p_z axis. This means that the corresponding rate for the angle θ_e is equal to the rate for the angle $2\beta_1 - \theta_e$. The parametric plot of the vector potential $\mathbf{A}(t)$ obeys reflection symmetry about axes at the angles $\beta_j = -\alpha_j/2 = jr180^\circ/(r+s)$ ($j = 0, \dots, r+s-1$) with respect to the positive A_z axis. In the atomic case, this leads to the general reflection symmetry of the direct ATI rate [40]. In Appendix A, we show that for linear molecules this symmetry holds for particular molecular orientation angles θ_L and the corresponding reflection-symmetry axes at the angles β_j , which, according to the relation (A2), are given by

$$\theta_L = j_3 90^\circ - \beta_j, \quad \beta_j = j \frac{r}{r+s} 180^\circ, \quad (13)$$

where $j_3 = \pm 1$ for asymmetric linear molecules. For symmetric linear molecules, relation (13) is valid also for $j_3 = 0$. Using Eq. (13), we can easily explain the result of Fig. 11: for the top panel we have $j_3 = j = 0$, $\theta_L = 0^\circ$, $\beta_0 = 0^\circ$; for the middle panel it is $j_3 = 1$, $j = 0$, $\theta_L = 90^\circ$, $\beta_0 = 0^\circ$; while for the bottom panel we get $j_3 = 1$, $j = 1$, $\beta_1 = 60^\circ$, $\theta_L = 90^\circ - 60^\circ = 30^\circ$.

As both j and j_3 can be positive or negative, from relation (13) one can conclude that the ATI spectra will observe reflection symmetry for molecular orientations (θ_L) perpendicular to the reflection axes (β_j) of the vector-potential curves. In Fig. 2, these perpendicular lines (molecular orientations) are represented by dashed lines. These lines coincide with the

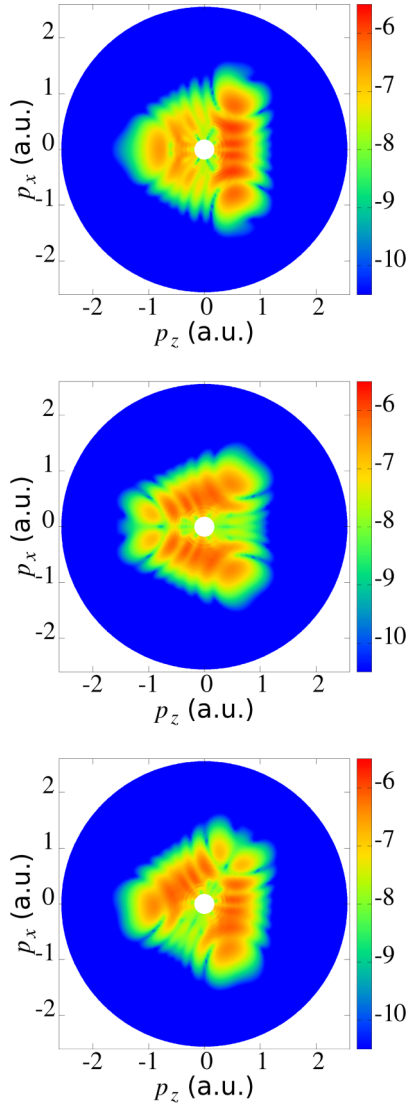


FIG. 11. Electron ATI spectra for the CO₂ molecule and the same laser-field parameters as in Fig. 6 for the orientations $\theta_L = 0^\circ$ (top panel), $\theta_L = 90^\circ$ (middle panel), and $\theta_L = 30^\circ$ (bottom panel). Each spectrum has one reflection-symmetry axis, and the spectra for $\theta_L = 90^\circ$ and 30° are related by a rotation.

reflection axes of the parametric plot of the electric field, and for even $r + s$ they also coincide with the reflection axes of the vector-potential curves (see the right-hand panel of Fig. 2). This can also be explained by a closer inspection of the values of the molecular orientations θ_L from relation (13). Similarly as was done for the relation (10), it can be shown that, for suitable odd j_3 , it is

$$\theta_L = j_3 90^\circ - \beta_j = \begin{cases} -\beta_{n'} + \frac{90^\circ}{r+s} & \text{for } r + s = 2k + 1, \\ -\beta_n & \text{for } r + s = 2k, \end{cases} \quad (14)$$

where $k, n = j - j_3 k / r$, and $n' = j - [j_3(2k + 1) - 1] / (2r)$ are integers. For symmetric molecules, where $j_3 = 0, \pm 1$ (or generally, any arbitrary integer due to the periodicity of the sine and cosine functions), for odd $r + s$ the angle θ_L takes on a different set of values for j_3 odd and for j_3 even, but for even $r + s$

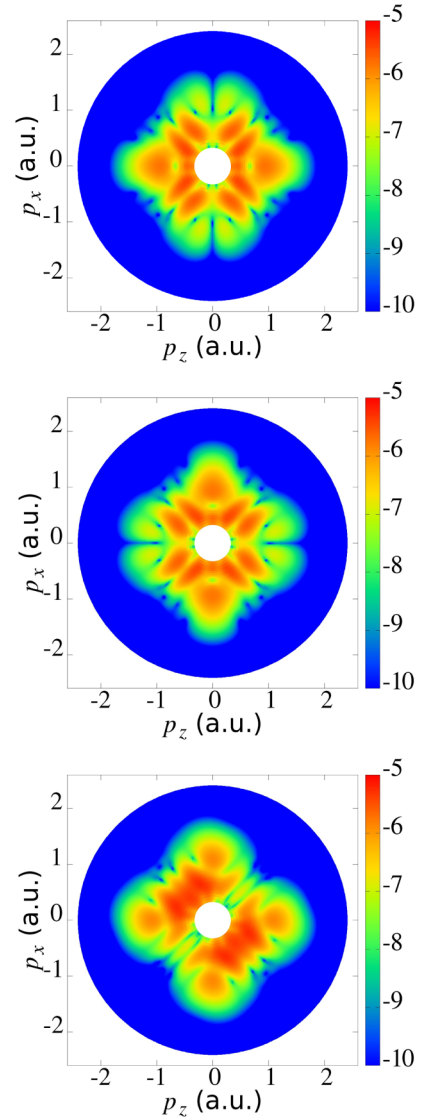


FIG. 12. Electron ATI spectra for a bicircular field with the same laser-field parameters as in Fig. 6 and for $r = 1$ and $s = 3$, for the O₂ molecule aligned at the angle $\theta_L = 0^\circ$ (top panel), $\theta_L = 90^\circ$ (middle panel), and $\theta_L = 45^\circ$ (bottom panel).

it acquires the same set of values in both cases. This is why for odd $r + s$ and a symmetric linear molecule there are additional orientations that lead to symmetric ATI spectra. For example, for $r = 1, s = 2$ and symmetric linear molecules [N₂ (see [60]), O₂, CO₂] there is reflection symmetry in the spectra for the orientation angles $\theta_L = 0^\circ, 30^\circ, 60^\circ, 90^\circ, 120^\circ, \dots$, while for asymmetric linear molecules (CO, OCS) we have reflection symmetry for the orientation angles $\theta_L = 30^\circ, 90^\circ, 150^\circ, \dots$

For a bicircular field with even $r + s$, we have shown that for symmetric molecules the spectrum satisfies inversion symmetry $\mathbf{p} \rightarrow -\mathbf{p}$ both for ATI and HATI electrons. An example of direct electron ATI spectra is shown in Fig. 12. In addition to this inversion symmetry, the spectra satisfy the reflection symmetry (13). This results in two mutually perpendicular reflection-symmetry axes. This can also be seen from relations (13) and (14) for even $r + s$, as there are two different reflection-symmetry-axis angles β_j for odd j_3

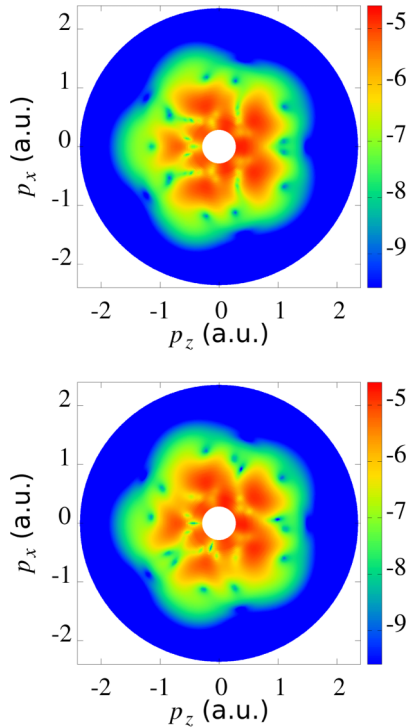


FIG. 13. Electron ATI spectra for the CO molecule and for a bicircular field with the same laser parameters as in Fig. 6, but for $r = 1$ and $s = 4$. Upper panel: $\theta_L = 90^\circ$. Lower panel: $\theta_L = 54^\circ$.

and β_n for $j_3 = 0$, which correspond to the same orientation θ_L . For the top panel of Fig. 12, we have $\theta_L = 0^\circ$ and two reflection-symmetry axes at the angles $\beta_0 = 0^\circ$ for $j_3 = 0$ and $\beta_{\pm 2} = \pm 90^\circ$ for $j_3 = \pm 1$. Similarly, for the middle panel ($\theta_L = 90^\circ$) we again have two angles: $\beta_0 = 0^\circ$ for $j_3 = 1$ and $\beta_{-2} = -90^\circ$ for $j_3 = 0$. Finally, for the bottom panel ($\theta_L = 45^\circ$) the corresponding angles are $\beta_{-1} = -45^\circ$ for $j_3 = 0$ and $\beta_1 = 45^\circ$ for $j_3 = 1$.

Examples of ATI electron spectra for asymmetric molecules are shown in Figs. 13 and 17. In Figs. 13 and 14, we present results for the CO molecule and the angles $\theta_L = 90^\circ$ and 54° . For $\theta_L = 90^\circ$ the reflection-symmetry axis is at the angle $\beta_0 = 0^\circ$, while for $\theta_L = 54^\circ$ we determine this angle in the following way. For $r = 1$ and $s = 4$ from Eq. (13) for $j_1 = j_3 = 1$ we obtain $\beta_1 = j_3 \times 90^\circ - \theta_L = 1 \times 90^\circ - 54^\circ = 36^\circ$, while for $r = 2$ and $s = 3$ and for $j_1 = -2$ and $j_3 = -1$ we get $\beta_{-2} = -1 \times 90^\circ - 54^\circ = -144^\circ$. These results are in accordance with the spectra presented in the lower panels of Figs. 13 and 14.

From Fig. 15 we see that the reflection symmetry is violated for $\theta_L = 0^\circ$ and the CO molecule. The absence of this symmetry can also be seen in the top panel of Fig. 16 for the OCS molecule. Due to the larger asymmetry in the electron density function for the CO molecule in comparison with the OCS molecule, the mentioned reflection-symmetry violation is more visible for the CO molecule. On the other hand, the ATI spectra shown in the middle panels of Figs. 15 and 16 confirm the symmetry with respect to the reflection $P_z(\theta_L = 90^\circ)$. The results presented in the bottom panels of Figs. 15 and 16 are in accordance with the relation (13) for $\theta_L = 30^\circ$, $j_3 = 1$, and $\beta_1 = 60^\circ$.

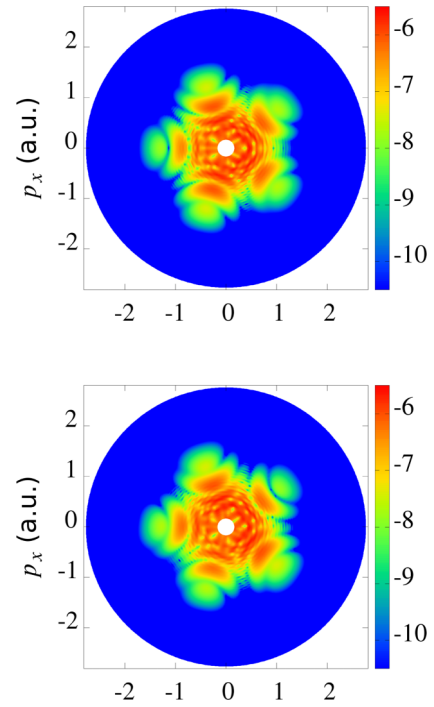


FIG. 14. Electron ATI spectra for the CO molecule and for a bicircular field having the intensity $E_L^2 = 1 \times 10^{14}$ W/cm², fundamental wavelength 1600 nm, $r = 2$, and $s = 3$. Upper panel: $\theta_L = 90^\circ$. Lower panel: $\theta_L = 54^\circ$.

Another example for the CO molecule and a bicircular field with $r = 1$ and $s = 3$ is presented in Fig. 17. It is obvious that for $\theta_L = 90^\circ$ (upper panel) the angle of the reflection-symmetry axis is $\beta_0 = 0^\circ$, which agrees with the relation (13) for $j_3 = 1$. However, contrary to the result for symmetric linear molecules, presented in the middle panel of Fig. 12, there is no symmetry axis for the angle $\beta_{-2} = -90^\circ$ since for asymmetric molecules relation (13) is not valid for $j_3 = 0$. Finally, for the lower panel of Fig. 17 for $\theta_L = 45^\circ$ we again have only one reflection symmetry axis for $\beta_1 = 45^\circ$ and $j_3 = 1$.

For molecular orientations that do not satisfy the criterion (13), there is no reflection symmetry for the direct ATI electron spectra. An example for the O₂ molecule with $\theta_L = 45^\circ$, for a bicircular field with $r = 1$ and $s = 2$, is presented in Fig. 18.

VI. CONCLUSIONS

In this paper, symmetries of ATI and HATI electron spectra of oriented linear molecules generated by a bicircular laser field are considered. Differences in these symmetries for asymmetric and symmetric linear molecules are examined and explained. In the general case of arbitrary linear molecules in a bicircular field with frequencies $r\omega$ and $s\omega$, the electron velocity maps exhibit rotational symmetry. We considered the case when the molecules are aligned perpendicular to the polarization plane and the case when they lie in the polarization plane. In the first case, the HATI spectra exhibit $(r + s)$ -fold rotational symmetry as in the atomic case, but with some additional interference pattern. This pattern is caused by the interference of electron wave packets released from different

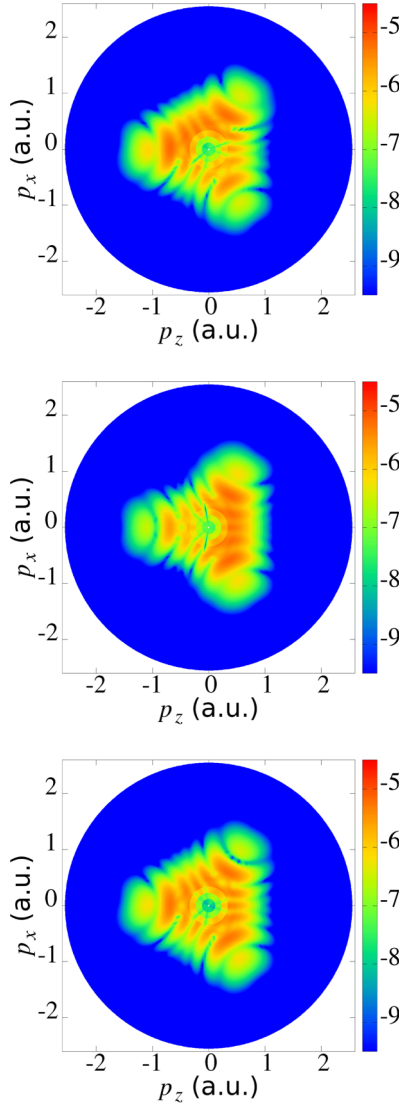


FIG. 15. Electron ATI spectra for the CO molecule and the same laser-field parameters as in Fig. 6 for the orientations $\theta_L = 0^\circ$ (top panel), $\theta_L = 90^\circ$ (middle panel), and $\theta_L = 30^\circ$ (bottom panel). There is no reflection symmetry for $\theta_L = 0^\circ$, but there is a reflection symmetry for the spectra for $\theta_L = 90^\circ$ and 30° , as shown in Appendix A.

atomic centers. In the second case, the electron velocity map for a molecule oriented by the angle θ_L in the polarization plane of the laser field is the same as the electron velocity map rotated by the angle $\alpha_{j_1} = -j_1 r 360^\circ / (r + s)$ (j_1 integer), for the same molecule but oriented by the angle $\theta_L - \alpha_{j_1}$.

In the remaining part of this section, we address the additional rotational and reflection symmetries for linear molecules oriented in the laser-field polarization plane. For symmetric linear molecules (compared with asymmetric molecules) there is an additional rotational symmetry with respect to rotation by the angle $j_2 180^\circ$ (j_2 integer) about an axis perpendicular to the polarization plane. For even $r + s$ this rotational symmetry manifests itself by a twofold symmetry, i.e., by the inversion symmetry ($\mathbf{p} \rightarrow -\mathbf{p}$). The curves of the corresponding electric field and vector potential exhibit the same inversion symmetry (see the right-hand panel of Fig. 2).

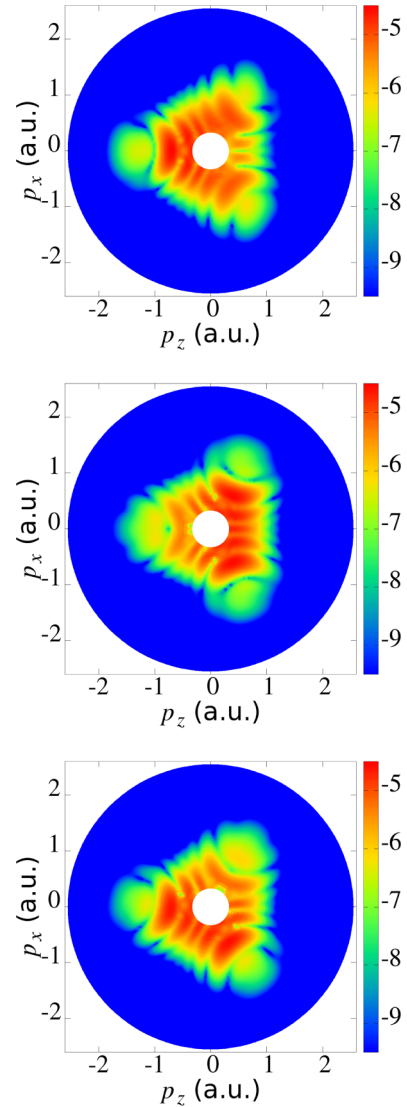


FIG. 16. Same as in Fig. 15 but for the OCS molecule.

On the other hand, for odd $r + s$ the electron spectrum in the direction of the angle θ_e for the molecular orientation angle θ_L is the same if it is rotated by the angle α_{j_1} , i.e., in the direction of the angle $\theta_e + \alpha_{j_1}$, but for the molecular orientation angle $\theta_L + j_2 180^\circ - \alpha_{j_1} = \theta_L - \alpha_{m'} + 180^\circ / (r + s) = \theta_L + (2rm' + 1)180^\circ / (r + s)$, where $m' = j_1 + [j_2(r + s) - 1] / (r + s)$. Here j_2 is an arbitrary odd integer, which can be chosen such that $\alpha_{m'} = 0$ [for example, for $m' = 0$ and $j_2 = 1$ compare Fig. 6 ($j_1 = -1$) and Fig. 7 ($j_1 = -2$)].

The direct ATI spectra for an atom in a bicircular field have $2(r + s)$ reflection-symmetry axes, which coincide with the reflection-symmetry axes of the vector potential $\mathbf{A}(t)$. These axes are determined by the angles $\beta_j = jr 180^\circ / (r + s) = -\alpha_j / 2$, $j = 0, 1, \dots, 2(r + s) - 1$, with respect to the positive z_L axis. The direct ATI spectra for arbitrary linear molecules that lie in the polarization plane and are oriented by the angle $\theta_L = j_3 90^\circ - \beta_j$, $j_3 = \pm 1$, have one reflection-symmetry axis, which is determined by the angle β_j . This means that in this case the spectrum is the same for the angles θ_e and $2\beta_j - \theta_e$. For easier visualization, these molecular orientations

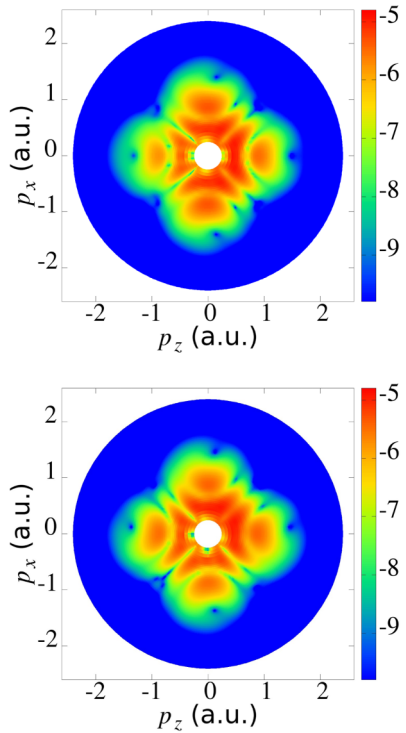


FIG. 17. Electron ATI spectra for a bicircular field with $r = 1$ and $s = 3$, for alignment $\theta_L = 90^\circ$ (upper panel) and $\theta_L = 45^\circ$ (lower panel) of the CO molecule, and other laser parameters as in Fig. 6.

are along the lines perpendicular to the reflection-symmetry axes of the vector potential $\mathbf{A}(t)$. In particular, for even $r + s$ these perpendicular lines are identical with the symmetry axes of the vector potential itself. The ATI spectra for other orientations in the polarization plane obey, in general, no symmetries at all.

For symmetric linear molecules, there is an additional reflection symmetry for $j_3 = 0$ in the upper formula (14), i.e., for the molecular orientation angle $\theta_L = -\beta_j$, with the corresponding reflection-symmetry axis at the angle β_j . For even $r + s$, this leads to ATI spectra with two mutually perpendicular reflection-symmetry axes for suitable molecular orientations θ_L , one at the angle $-\theta_L$ and another one at the

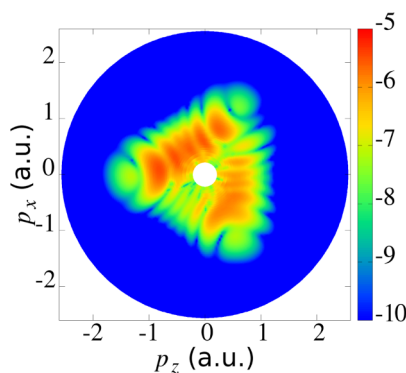


FIG. 18. Electron ATI spectra in the momentum plane for the O_2 molecule oriented by the angle $\theta_L = 45^\circ$ and the same laser parameters as in Fig. 6.

angle $90^\circ - \theta_L$. When $r + s$ is odd, we get another set of orientations that will produce ATI spectra having reflection symmetries [these orientations coincide with the reflection-symmetry axes of the vector potential $\mathbf{A}(t)$].

Finally, while some symmetries of the photoelectron spectra are immediately related to the symmetry of the laser field and look obvious, some others are not easy to find. In this sense, the careful analysis presented in this paper is indispensable for applications. Possible applications are numerous. At the end of Sec. III we mentioned checking the degree of linearity of the molecule and, for linear molecules, its alignment. One can also extract elastic-scattering differential cross sections of the molecular targets [57] in a similar way as was done for atomic targets exposed to the bicircular field in Ref. [43]. More applications are waiting to be discovered.

The rotational symmetries also hold for the exact ionization amplitude, regardless of the SFA or ISFA, provided the laser pulse is long enough. So they should be observed by solutions of the time-dependent Schrödinger equation (TDSE) and, ultimately, by experimental data. The reflection symmetries, on the other hand, only hold for the direct (ATI) electrons. The extent to which they are visible in realistic simulations (TDSE or experimental data) allows one to assess the importance of rescattering contributions.

ACKNOWLEDGMENTS

Support by the Federal Ministry of Education and Science, Bosnia and Herzegovina, is gratefully acknowledged. This work was also supported in part by the Deutsche Forschungsgemeinschaft within the Priority Programme Quantum Dynamics in Tailored Intense Fields (QUTIF).

APPENDIX: INVARIANCE OF THE DIRECT DIFFERENTIAL IONIZATION RATE WITH RESPECT TO THE REFLECTION TRANSFORMATIONS

In Appendix C of Ref. [60], we proved that the differential ionization rate of direct ATI is invariant with respect to the reflections $\hat{\mathbf{x}} \rightarrow -\hat{\mathbf{x}}$ (for fixed angle $\theta_L = 0^\circ$) and $\hat{\mathbf{z}} \rightarrow -\hat{\mathbf{z}}$ (for fixed angle $\theta_L = 90^\circ$). The corresponding operators of these reflections were denoted by $P_x(\theta_L = 0^\circ)$ and $P_z(\theta_L = 90^\circ)$, while the transformed quantities were denoted by a double prime and a triple prime, respectively. In the proof of the invariance under the reflection $P_x(\theta_L = 0^\circ)$, we used the fact that for homonuclear diatomic molecules the expansion coefficients c_{qa} and c_{-qa} of the ground-state molecular wave function in terms of the atomic orbitals are equal up to a sign. For heteronuclear diatomic molecules this is no longer the case, and the corresponding differential ionization rate is not invariant with respect to this transformation. However, it is invariant with respect to the second transformation $P_z(\theta_L = 90^\circ)$, which we will show in the remaining part of this Appendix.

In Ref. [52], we have shown that the term $q = \pm 1$ for heteronuclear molecules should be replaced by $q - \lambda$, where λ is the mass asymmetry parameter. Taking into account that for heteronuclear molecules we dress the whole molecular orbital and not the atomic centers, we can repeat the derivation of Appendix C of Ref. [60], replacing $q\mathbf{p} \cdot \mathbf{R}/2$ with $(q - \lambda)[\mathbf{p} + \mathbf{A}(t)] \cdot \mathbf{R}/2 + \mu_S(t) + \alpha_S(t)$. For heteronuclear molecules, we

should consider how the molecular-dipole term and the polarizability term change under the reflection $\hat{\mathbf{z}} \rightarrow -\hat{\mathbf{z}}$. The molecular dipole $\boldsymbol{\mu} = -\mu\hat{\mathbf{z}}$ is oriented along the internuclear axis so that this transformation changes its sign, i.e., $\boldsymbol{\mu} \rightarrow -\boldsymbol{\mu}$. The reflection transformation for the time-dependent dipole gives $\mu_S'''(t) = -\int^{(-t)}(-\boldsymbol{\mu}) \cdot [-\mathbf{E}(\boldsymbol{\tau})]d\boldsymbol{\tau} = -\mu_S(-t)$. Analogously, for the polarizability term we obtain $\alpha_S'''(t) = -\alpha_S(-t)$. Using this and the transformation properties of the atomic wave functions $\psi_a(-\mathbf{r}) = (-1)^{m_a}\psi_a(\mathbf{r}'')$, we obtain

$$T_{\mathbf{R}\mathbf{p}_i}^{(0)}(n) = (-1)^{m_a} [T_{\mathbf{R}\mathbf{p}''_i}^{(0)}(n)]^*. \quad (\text{A1})$$

From this we get the required result $w_{\mathbf{R}\mathbf{p}_i}^{(0)}(n) = w_{\mathbf{R}\mathbf{p}''_i}^{(0)}(n)$. Analogous considerations are valid for any linear asymmetric molecule, say OCS.

Since the matrix elements of the 2×2 reflection matrix are the same for the angles $\theta_L = 90^\circ$ and -90° , i.e., $[P_z(\pm 90^\circ)]_{11} = -[P_z(\pm 90^\circ)]_{22} = -1$ and $[P_z(\pm 90^\circ)]_{12} = [P_z(\pm 90^\circ)]_{21} = 0$ [40], the reflection symmetry derived above is valid also for the angle $\theta_L = -90^\circ$. We can express all these reflection symmetries by the relation

$$\theta \rightarrow j_3 180^\circ - \theta, \quad \theta_L = j_3 90^\circ, \quad \theta_e \rightarrow -\theta_e \quad (j_3 = 0, \pm 1). \quad (\text{A2})$$

The reflection symmetry for $j_3 = \pm 1$ is valid for all linear molecules, while the symmetry for $j_3 = 0$ is valid only if they are symmetric.

The result (A2) can be further generalized. It can be shown that the differential ionization rate for the molecular orientation angle $\theta_L = j_3 90^\circ - \beta_j$, $j_3 = 0, \pm 1$, j an integer, is invariant with respect to the reflection about a line through the origin that makes an angle β_j with respect to the z_L axis, i.e.,

$$w_{\mathbf{R}\mathbf{p}_i}^{(0)}(n) = w_{\tilde{\mathbf{R}}\tilde{\mathbf{p}}_i}^{(0)}(n), \quad \tilde{\mathbf{p}} = P_{z_L}(\beta_j)\mathbf{p}, \quad \theta_L = j_3 90^\circ - \beta_j. \quad (\text{A3})$$

Here the reflection operator $P_{z_L}(\beta_j)$ and the angle $\beta_j = -\alpha_j/2 = jr\pi/(r+s)$ were defined in Ref. [40]. According to Eq. (40), from this reference we have $\tilde{\mathbf{E}}(t) = -\mathbf{E}(\tau_j - t)$, $\tilde{\mathbf{A}}(t) = \mathbf{A}(\tau_j - t)$, and $\tilde{\boldsymbol{\alpha}}(t) = -\boldsymbol{\alpha}(\tau_j - t)$. The angle between the z axis, which is in the direction \mathbf{R} , and the reflection-symmetry axis is $\theta_L + \beta_j = j_3 90^\circ$, so that for $j_3 = \pm 1$ it is $\tilde{\mathbf{R}} = -\mathbf{R}$, while for $j_3 = 0$ it is $\tilde{\mathbf{R}} = \mathbf{R}$. Using this, we can repeat the derivation of Appendix C from Ref. [60] and obtain the result (A3). One should also have in mind that $P_x(\theta_L = 0^\circ) = P_{z_L}(0^\circ)$.

-
- [1] H. Eichmann, A. Egbert, S. Nolte, C. Momma, B. Wellegehausen, W. Becker, S. Long, and J. K. McIver, *Phys. Rev. A* **51**, R3414 (1995).
- [2] S. Long, W. Becker, and J. K. McIver, *Phys. Rev. A* **52**, 2262 (1995).
- [3] T. Zuo and A. D. Bandrauk, *J. Nonlin. Opt. Phys. Mater.* **04**, 533 (1995).
- [4] D. B. Milošević, W. Becker, and R. Kopold, *Phys. Rev. A* **61**, 063403 (2000).
- [5] D. B. Milošević and W. Sandner, *Opt. Lett.* **25**, 1532 (2000).
- [6] D. B. Milošević, W. Becker, R. Kopold, and W. Sandner, *Laser Phys.* **11**, 165 (2001).
- [7] D. B. Milošević and W. Becker, *Phys. Rev. A* **62**, 011403(R) (2000); *J. Mod. Opt.* **52**, 233 (2005).
- [8] D. B. Milošević, W. Becker, and R. Kopold, in *Atoms, Molecules and Quantum Dots in Laser Fields: Fundamental Processes*, edited by N. Bloembergen, N. Rahman, and A. Rizzo, Conference Proceedings Vol. 71 (Società Italiana di Fisica, Bologna, 2001), pp. 239–252.
- [9] A. Fleischer, O. Kfir, T. Diskin, P. Sidorenko, and O. Cohen, *Nat. Photon.* **8**, 543 (2014).
- [10] E. Pisanty, S. Sukiasyan, and M. Ivanov, *Phys. Rev. A* **90**, 043829 (2014).
- [11] O. Kfir *et al.*, *Nat. Photon.* **9**, 99 (2015).
- [12] T. Fan *et al.*, *Proc. Natl. Acad. Sci. USA* **112**, 14206 (2015).
- [13] D. B. Milošević, *Phys. Rev. A* **92**, 043827 (2015); *Opt. Lett.* **40**, 2381 (2015); *J. Phys. B* **48**, 171001 (2015).
- [14] S. Odžak and D. B. Milošević, *Phys. Rev. A* **92**, 053416 (2015).
- [15] L. Medišauskas, J. Wragg, H. van der Hart, and M. Yu. Ivanov, *Phys. Rev. Lett.* **115**, 153001 (2015).
- [16] C. Chen *et al.*, *Sci. Adv.* **2**, e1501333 (2016).
- [17] D. B. Milošević, *Phys. Rev. A* **93**, 051402(R) (2016); *J. Phys. B* **50**, 164003 (2017).
- [18] D. Baykusheva, M. S. Ahsan, N. Lin, and H. J. Wörner, *Phys. Rev. Lett.* **116**, 123001 (2016).
- [19] F. Mauger, A. D. Bandrauk, and T. Uzer, *J. Phys. B* **49**, 10LT01 (2016).
- [20] H. Du, J. Zhang, S. Ben, H.-Y. Zhong, T.-T. Xu, J. Guo, and X.-S. Liu, *Chin. Phys. B* **25**, 043202 (2016).
- [21] X. Liu, X. Zhu, L. Li, Y. Li, Q. Zhang, P. Lan, and P. Lu, *Phys. Rev. A* **94**, 033410 (2016).
- [22] S. Odžak, E. Hasović, and D. B. Milošević, *Phys. Rev. A* **94**, 033419 (2016).
- [23] D. M. Reich and L. B. Madsen, *Phys. Rev. Lett.* **117**, 133902 (2016).
- [24] E. Hasović, S. Odžak, W. Becker, and D. B. Milošević, *Mol. Phys.* **115**, 1750 (2017).
- [25] K. M. Dorney, J. L. Ellis, C. Hernandez-Garcia, D. D. Hickstein, C. A. Mancuso, N. Brooks, T. Fan, G. Fan, D. Zusin, C. Gentry, P. Grychtol, H. C. Kapteyn, and M. M. Murnane, *Phys. Rev. Lett.* **119**, 063201 (2017).
- [26] D. Ayuso, A. Jiménez-Galán, F. Morales, M. Ivanov, and O. Smirnova, *New J. Phys.* **19**, 073007 (2017).
- [27] N. Zhavoronkov and M. Ivanov, *Opt. Lett.* **42**, 4720 (2017).
- [28] D. B. Milošević, *Phys. Rev. A* **97**, 013416 (2018).
- [29] L. V. Keldysh, *Zh. Eksp. Teor. Fiz.* **47**, 1945 (1964) [*Sov. Phys. JETP* **20**, 1307 (1965)].
- [30] T. Zuo, A. D. Bandrauk, and P. B. Corkum, *Chem. Phys. Lett.* **259**, 313 (1996).
- [31] M. Spanner, O. Smirnova, P. B. Corkum, and M. Y. Ivanov, *J. Phys. B* **37**, L243 (2004).

- [32] M. Meckel, D. Comtois, D. Zeidler, A. Staudte, D. Pavičić, H. C. Bandulet, H. Pépin, J. C. Kieffer, R. Dörner, D. M. Villeneuve, and P. B. Corkum, *Science* **320**, 1478 (2008).
- [33] C. I. Blaga, J. Xu, A. D. DiChiara, E. Sistrunk, K. Zhang, P. Agostini, T. A. Miller, L. F. DiMauro, and C. D. Lin, *Nature (London)* **483**, 194 (2012).
- [34] W. Becker, F. Grasbon, R. Kopold, D. B. Milošević, G. G. Paulus, and H. Walther, *Adv. At. Mol. Opt. Phys.* **48**, 35 (2002).
- [35] E. Hasović, D. B. Milošević, and W. Becker, *Laser Phys. Lett.* **3**, 200 (2006).
- [36] A. Kramo, E. Hasović, D. B. Milošević, and W. Becker, *Laser Phys. Lett.* **4**, 279 (2007).
- [37] E. Hasović, A. Kramo, and D. B. Milošević, *Eur. Phys. J. Spec. Top.* **160**, 205 (2008).
- [38] C. A. Mancuso, D. D. Hickstein, P. Grychtol, R. Knut, O. Kfir, X. M. Tong, F. Dollar, D. Zusin, M. Gopalakrishnan, C. Gentry, E. Turgut, J. L. Ellis, M. C. Chen, A. Fleischer, O. Cohen, H. C. Kapteyn, and M. M. Murnane, *Phys. Rev. A* **91**, 031402(R) (2015).
- [39] E. Hasović, W. Becker, and D. B. Milošević, *Opt. Express* **24**, 6413 (2016).
- [40] D. B. Milošević and W. Becker, *Phys. Rev. A* **93**, 063418 (2016).
- [41] C. A. Mancuso, D. D. Hickstein, K. M. Dorney, J. L. Ellis, E. Hasović, R. Knut, P. Grychtol, C. Gentry, M. Gopalakrishnan, D. Zusin, F. J. Dollar, X. M. Tong, D. B. Milosevic, W. Becker, H. C. Kapteyn, and M. M. Murnane, *Phys. Rev. A* **93**, 053406 (2016).
- [42] S. Odžak, E. Hasović, W. Becker, and D. B. Milošević, *J. Mod. Opt.* **64**, 971 (2017).
- [43] V.-H. Hoang, V.-H. Le, C. D. Lin, and A.-T. Le, *Phys. Rev. A* **95**, 031402(R) (2017).
- [44] D. B. Milošević and W. Becker, *J. Phys. B* **51**, 054001 (2018).
- [45] D. B. Milošević, *Phys. Rev. A* **74**, 063404 (2006).
- [46] M. Busuladžić and D. B. Milošević, *Phys. Rev. A* **82**, 015401 (2010).
- [47] F. Grasbon, G. G. Paulus, S. L. Chin, H. Walther, J. Muth-Böhm, A. Becker, and F. H. M. Faisal, *Phys. Rev. A* **63**, 041402(R) (2001).
- [48] M. Busuladžić, A. Gazibegović-Busuladžić, D. B. Milošević, and W. Becker, *Phys. Rev. Lett.* **100**, 203003 (2008).
- [49] M. Busuladžić, A. Gazibegović-Busuladžić, D. B. Milošević, and W. Becker, *Phys. Rev. A* **78**, 033412 (2008).
- [50] M. Busuladžić, A. Gazibegović-Busuladžić, and D. B. Milošević, *Phys. Rev. A* **80**, 013420 (2009).
- [51] M. Busuladžić, A. Gazibegović-Busuladžić, W. Becker, and D. B. Milošević, *Eur. Phys. J. D* **67**, 61 (2013).
- [52] E. Hasović, M. Busuladžić, W. Becker, and D. B. Milošević, *Phys. Rev. A* **84**, 063418 (2011).
- [53] M. Busuladžić, E. Hasović, W. Becker, and D. B. Milošević, *J. Chem. Phys.* **137**, 134307 (2012).
- [54] E. Hasović and D. B. Milošević, *Phys. Rev. A* **89**, 053401 (2014).
- [55] M. Okunishi, R. Itaya, K. Shimada, G. Prümper, K. Ueda, M. Busuladžić, A. Gazibegović-Busuladžić, D. B. Milošević, and W. Becker, *J. Phys. B* **41**, 201004 (2008).
- [56] M. Okunishi, R. Itaya, K. Shimada, G. Prümper, K. Ueda, M. Busuladžić, A. Gazibegović-Busuladžić, D. B. Milošević, and W. Becker, *Phys. Rev. Lett.* **103**, 043001 (2009).
- [57] A. Gazibegović-Busuladžić, E. Hasović, M. Busuladžić, D. B. Milošević, F. Kelkensberg, W. K. Siu, M. J. J. Vrakking, F. Lépine, G. Sansone, M. Nisoli, I. Znakovskaya, and M. F. Kling, *Phys. Rev. A* **84**, 043426 (2011).
- [58] W. Quan, X.-Y. Lai, Y.-J. Chen, C.-L. Wang, Z.-L. Hu, X.-J. Liu, X.-L. Hao, J. Chen, E. Hasović, M. Busuladžić, W. Becker, and D. B. Milošević, *Phys. Rev. A* **88**, 021401(R) (2013).
- [59] W. Quan, X.-Y. Lai, Y.-J. Chen, C.-L. Wang, Z.-L. Hu, X.-J. Liu, X.-L. Hao, J. Chen, E. Hasović, M. Busuladžić, D. B. Milošević, and W. Becker, *Chin. J. Phys.* **52**, 389 (2014).
- [60] M. Busuladžić, A. Gazibegović-Busuladžić, and D. B. Milošević, *Phys. Rev. A* **95**, 033411 (2017).
- [61] E. Hasović and D. B. Milošević, *Phys. Rev. A* **86**, 043429 (2012).
- [62] L. F. DiMauro and P. Agostini, *Adv. At. Mol. Opt. Phys.* **35**, 79 (1995); E. Hasović, M. Busuladžić, A. Gazibegović-Busuladžić, D. B. Milošević, and W. Becker, *Laser Phys.* **17**, 376 (2007).